Ring-Laser Mode Coupling

CYNTHIA WHITNEY
Instrumentation Laboratory, Massachusetts Institute of Technology, Cambridge, Massachusetts 02142
(Received 27 September 1968)

Fundamentals of the physics of continuous-wave gas ring lasers, summarized in the preceding paper, are used to establish a model of mode coupling in the limit of low excitation. It predicts a steady state with each traveling wave composed of radiation at two frequencies, both displaced by the coupling from the cavity resonant frequency. Inter- and intrawave instantaneous and time-average beat frequencies are computed.

1. BACKGROUND

A RING laser supporting oscillation in a single, fundamental, longitudinal, polarized mode is considered. The electromagnetic fields are treated as a combination of forward (F) and backward (B) traveling plane waves, where forward is defined as the direction of any physical rotation of the ring about its axis. Let a general subscript S denote F or B. The wave numbers present are given by

$$K_S=2n\pi/l_S, \tag{1.1}$$

where n is an integer and l_S is the effective optical path length measured in the same coordinate frame as the corresponding wave number. The lengths can be predicted by the special theory of relativity, which postulates that light travels at speed c in empty, inertial space. It follows[1] that if the F and B waves are observed in a frame attached to the rotating ring, and if dispersion is neglected, the waves should be separated in frequency by an amount f_B proportional in first order to rotation rate ω_r:

$$f_B=2R\omega_r/\lambda. \tag{1.2}$$

The factor R has the dimension of length and is determined as twice the area of the ring divided by its inertial-space optical path length l. The factor λ is the wavelength of the radiation, l/n.

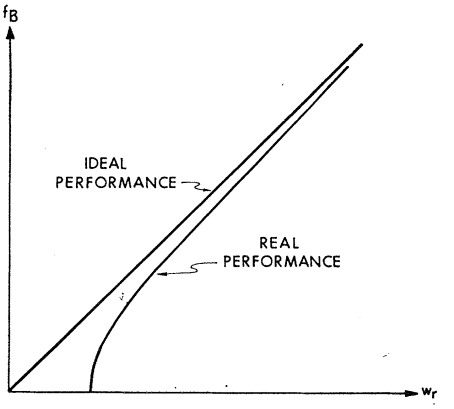

FIG. 1. Experimental ring-laser beat frequency f_B as a function of rotation rate ω_r.

One experimental effect encountered early in investigations of such rings is a nonlinearity of the measured time-average beat frequency f_B as a function of rotation rate ω_r. A typical curve of f_B versus ω_r is shown in Fig. 1. At sufficiently low rotation rates, f_B disappears completely. This so-called lock-in has been explained in terms of coupling of the F and B waves through scattering of radiation within the laser cavity; theoretical formulations of the mechanism based on nonlinear differential equations have been discussed by many authors.[2–9]

A different type of analysis suggests itself as follows: One postulates that the fields achieve the steady state described in the preceding paper in terms of autocorrelations. Let the field spatial Fourier amplitudes be time-Fourier-decomposed. The resulting amplitude distribution satisfies a self-consistency equation similar to that first introduced by Lamb[10] and later extended by Aronowitz[11] to the case of the ring laser; it is shown in Appendix C. No matter what the time decomposition is, for sufficiently low excitation, pulsations in the excitation density and gain are negligibly small compared to the total gain, making it approximately time-invariant. Furthermore, when the time decomposition contains only frequencies separated by much less than a linewidth, the gain is also nearly frequency-independent. It is then interesting to derive all the implications of a model assuming gain *exactly* time-invariant and frequency-independent. In the following sections, the predictions of such a linear model are derived. The frequency-domain techniques of linear system theory are used. Time-invariant rotation rate is considered. The required gains, the frequencies present, and the relative

[1] M. P. Langevin, Compt. Rend. **173**, 831 (1921).

[2] F. Aronowitz and R. J. Collins, Appl. Phys. Letters **9**, 55 (1966).

[3] C. C. Wang, in *Proceedings of the Symposium on Modern Optics* (Polytechnic Press, Brooklyn, New York, 1967); Sperry Gyroscope Co. Report No. AB-1272-0070, 1966 (unpublished).

[4] Yu. L. Klimontovich, V. N. Kuryatov, and P. S. Landa, Zh. Eksperim. i Teor. Fiz. **51**, 3 (1966) [English transl.: Soviet Phys.—JETP **24**, 1 (1967)].

[5] B. L. Zhelnov, A. P. Kazantsev, and V. S. Smirnov, Zh. Eksperim. i Teor. Fiz. **50**, 1291 (1960) [English transl.: Soviet Phys.—JETP **23**, 858 (1966)].

[6] S. G. Zeiger and E. E. Fradkin, Opt. i Spektroskopiya **21**, 386 (1966) [English transl.: Opt. Spectry. (USSR) **21**, 217 (1966)].

[7] H. deLang, Appl. Phys. Letters **9**, 205 (1965).

[8] C. L. Tang and H. Statz, J. Appl. Phys. **38**, 323 (1967).

[9] F. Bertein and F. Petit, Compt. Rend. **259**, 2980 (1964).

[10] W. E. Lamb, Jr., Phys. Rev. **134**, A1429 (1964).

[11] F. Aronowitz, Phys. Rev. **139**, A635 (1965).

amplitudes at each of the various frequencies are all computed. The observable beat frequency as a function of rotation rate is discussed. One alternative differential-equation analysis suitable for regions where the assumptions fail, namely, below and very far above lock-in, is described.

Linear techniques have previously been used to advantage in laser problems by authors such as Bertein and Petit,[9] Kumagai and Yamamoto,[12] and Fontana.[13] Because of their considerable simplicity, linear techniques can give substantial insight about the system being described.

2. COUPLED OSCILLATOR EQUATIONS

Several mechanisms couple the F and B modes in a ring laser. The gain experienced by each mode has some dependence on the amplitude of the wave in the other mode by virtue of the competition for those excited states of the laser population which can contribute to either gain.[4–8] By a proper choice of isotope concentrations and mean-mode frequency, this coupling can practically be eliminated.[14] A more persistent mode coupling results from reflection and scattering processes. Radiation backscattered from one mode constitutes an input to the other mode that can be amplified and perpetuated. A nonrotating inertial frame of reference is chosen for analysis of the latter coupling mechanism. In the absence of coupling, the F and B modes oscillate at optical frequencies Ω_{0F} and Ω_{0B} set by the dimensions of the cavity and the mode dispersions such that the corresponding wave vectors satisfy Eq. (1.1). For simplicity it is assumed that $\Omega_{0F}=\Omega_{0B}=\Omega_0$, although the assumption could easily be removed. In addition, low excitation is assumed, so that dispersion is unaltered by changes in intensities and frequencies caused by coupling, and Ω_0 is a constant in the analysis. A steady-state model of the uncoupled F or B mode as a linear system comprises a pair of complex-conjugate poles located in the frequency domain at $\pm i\Omega_0$. Since optical frequencies are so large, the separation of those conjugate poles is very large compared to any displacements of poles, frequency shifts, cavity bandwidths, or spectral linewidths to be expected in the analysis of the coupled problem. Therefore, the discussion is limited to poles in the upper half-plane and positive frequency components of the various signals.

The coupled F and B modes are modeled with single poles p_F and p_B, the exact locations of which are determined in Sec. 3. An input signal to the F mode with Fourier-transform amplitude $a_F(\Omega)$ induces a cavity wave with Fourier-transform amplitude

$$A_F(\Omega)=a_F(\Omega)/(i\Omega-p_F), \tag{2.1a}$$

and similarly for the B mode,

$$A_B(\Omega)=a_B(\Omega)/(i\Omega-p_B). \tag{2.1b}$$

The general amplitudes A and a can stand for electric fields or magnetic fields, or any convenient combination thereof.

The inputs to each mode are related to the losses from the opposite modes. The signal losses per unit time are shown in Appendix A to be

$$\tfrac{1}{2}\Delta\Omega_S A_S(t), \tag{2.2}$$

where $\Delta\Omega_F$ and $\Delta\Omega_B$ are passive cavity bandwidths.

The fractions of the signal losses that act as inputs to the opposite modes are designated as

$$S_S. \tag{2.3}$$

They can be estimated as the square roots of the intensity fractions backscattered into the area of the laser beam spot. Neglecting effects of mirror curvature, the spot area is approximately[15] λl. Suppose, for example, that the mirror scatters light uniformly in all directions. Then the intensity fraction is the spot area divided by the area of comparable sphere:

$$\lambda l/4\pi l^2=\lambda/4\pi l.$$

The fractions S_S are then approximately

$$S_S=(\lambda/4\pi l)^{1/2}.$$

Scattered radiation generally experiences a phase shift. The effects of the three or more mirrors in the ring laser are represented by single phase-shift angles

$$\phi_{FB} \quad \text{and} \quad \phi_{BF} \tag{2.4}$$

for B to F and F to B scattering, respectively.

If the ring laser is rotating about its axis, then in an inertial frame frequency shifts appear at backscattering. For all rotation rates of practical concern, the relative frequency shifts are very small, and are given in Appendix B as

$$|\delta\Omega/\Omega_0|\simeq 2R\omega_r/c. \tag{2.5}$$

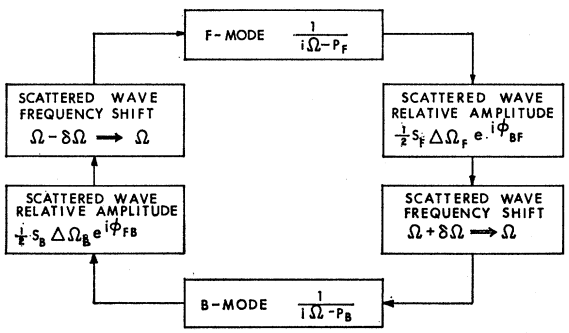

FIG. 2. Ring-laser mode-coupling model.

[12] N. Kumagai and H. I. Yamamoto, IEEE Trans. Microwave Theory Tech. **MTT 13**, 445 (1965).

[13] J. R. Fontana, IEEE Trans. Microwave Theory Tech. **MTT 12**, 400 (1964).

[14] J. D. Coccoli (private communication).

[15] G. D. Boyd and J. P. Gordon, Bell System Tech. J. **40**, 489 (1961).

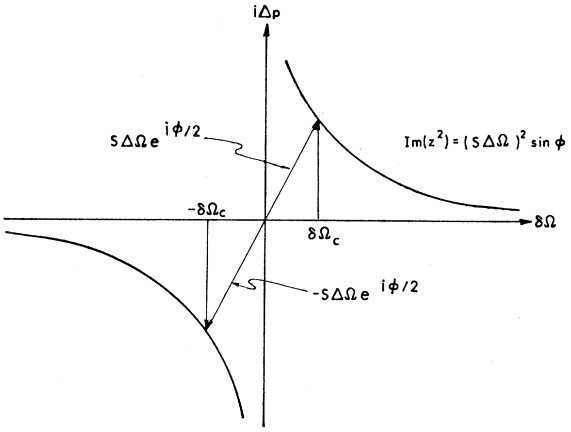

FIG. 3. Evaluation of Δp for given $S\Delta\Omega$, ϕ, and various $\delta\Omega$.

Shifts are positive for B to F scattering and negative for F to B.

When (2.2)–(2.5) are combined under the assumption that ω_r and $\delta\Omega$ are time-invariant, the F and B input-signal amplitudes are found as

$$a_S(\Omega)=\tfrac{1}{2}S_{S'}\Delta\Omega_{S'}e^{i\phi_{SS'}}A_{S'}(\Omega\mp\delta\Omega). \tag{2.6}$$

(Throughout the paper, subscript $S'\neq S$, and where double signs appear, the upper one corresponds to $S=F$, the lower to $S=B$.)

Figure 2 shows the F and B mode-coupling mechanism as a closed-loop system. Note that this system is not really linear, since the operations $\Omega-\delta\Omega\rightarrow\Omega$ and $\Omega+\delta\Omega\rightarrow\Omega$ are accomplished through multiplication by $e^{i\delta\Omega t}$ and $e^{-i\delta\Omega t}$, respectively. This feature does not, however, lead to any difficulty in formulating the coupled oscillator frequency domain equations, which are found from (2.1) and (2.6), or from Fig. 2, as

$$A_F(\Omega)=S_B\Delta\Omega_B e^{i\phi_{FB}}A_B(\Omega-\delta\Omega)/2(i\Omega-p_F) \tag{2.7a}$$

and

$$A_B(\Omega)=S_F\Delta\Omega_F e^{i\phi_{BF}}A_F(\Omega+\delta\Omega)/2(i\Omega-p_B). \tag{2.7b}$$

3. IMPLICATIONS OF THE COUPLED OSCILLATOR EQUATIONS

The following simplifying assumptions are employed: (a) The backscattered fractions are equal;

$$S_F=S_B=S.$$

(b) The F and B bandwidths are equal;

$$\Delta\Omega_F=\Delta\Omega_B=\Delta\Omega.$$

The characteristic frequencies of the coupled oscillator system are found as follows. In (2.7b), Ω is replaced by $\Omega-\delta\Omega$, and in (2.7a), Ω is replaced by $\Omega+\delta\Omega$, giving

$$A_B(\Omega-\delta\Omega)=S\Delta\Omega e^{i\phi_{BF}}A_F(\Omega)/2(i\Omega-i\delta\Omega-p_B) \tag{3.1a}$$

and

$$A_F(\Omega+\delta\Omega)=S\Delta\Omega e^{i\phi_{FB}}A_B(\Omega)/2(i\Omega+i\delta\Omega-p_F). \tag{3.1b}$$

Equation (3.1a) is substituted in (2.7a), Eq. (3.1b) in (2.7b), giving

$$A_F(\Omega)=(S\Delta\Omega)^2e^{i\phi}A_F(\Omega)/4(i\Omega-p_F)(i\Omega-i\delta\Omega-p_B), \tag{3.2a}$$

$$A_B(\Omega)=(S\Delta\Omega)^2e^{i\phi}A_B(\Omega)/4(i\Omega-p_B)(i\Omega+i\delta\Omega-p_F), \tag{3.2b}$$

where

$$\phi=\phi_{FB}+\phi_{BF}. \tag{3.2c}$$

The amplitudes in Eqs. (3.2a) and (3.2b) are cancelled and the resulting quadratic equations for the characteristic frequencies are solved, giving

$$\Omega_{S1}=\tfrac{1}{2}(-i\textstyle\sum p\pm\delta\Omega\mp\Re) \tag{3.3a}$$

and

$$\Omega_{S2}=\tfrac{1}{2}(-i\textstyle\sum p\pm\delta\Omega\pm\Re), \tag{3.3b}$$

where

$$\textstyle\sum p=p_F+p_B,$$
$$\Re=[(\delta\Omega+i\Delta p)^2-(S\Delta\Omega)^2e^{i\phi}]^{1/2}, \tag{3.3c}$$
$$\Delta p=p_F-p_B.$$

The characteristic frequencies are all distinct from the poles, as is typical even of coupled *lossless, gainless* oscillators. It is interesting that each mode has not one but *two* characteristic frequencies associated with it. This occurs because the F and B modes are not the *normal* modes of the coupled system. Note also that the two characteristic frequencies in the F mode are numerically unequal to those in the B mode. Thus, there are four distinct characteristic frequencies in the coupled system. Typically, two single-pole oscillators when coupled yield a system with only *two* distinct characteristic frequencies. This somewhat unusual four-frequency system follows the more typical pattern when viewed in a frame of reference attached to the rotating ring, where the characteristic frequencies become

$$\Omega_{RS1}=\tfrac{1}{2}(-i\textstyle\sum p\mp\Re) \tag{3.4a}$$

and

$$\Omega_{RS2}=\tfrac{1}{2}(-i\textstyle\sum p\pm\Re). \tag{3.4b}$$

The poles and characteristic frequencies can be specified as follows. First, steady state is assumed, constraining the characteristic frequencies to be real. Thus,

$$\mathrm{Re}\textstyle\sum p=0, \tag{3.5a}$$

$$\mathrm{Im}\Re=0, \tag{3.5b}$$

where Re and Im denote real and imaginary parts, respectively. Gains adjust to compensate for coupling. Thus the poles take the form

$$p_F=i\Omega_0-\gamma_F,$$
$$p_B=i\Omega_0-\gamma_B. \tag{3.6}$$

Equations (3.5a) and (3.6) imply that

$$\textstyle\sum p=2i\Omega_0, \tag{3.7a}$$

$$\gamma_F=-\gamma_B. \tag{3.7b}$$

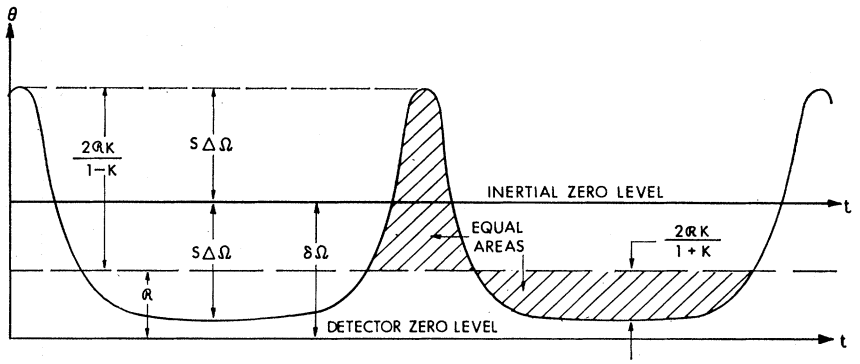

FIG. 4. Phase variation between B and F signals for $S\Delta\Omega/\delta\Omega\approx 0.90$. Note $\kappa=|\kappa_S|$.

It is interesting that the assumed *stability* of signals present implies one *negative* γ. The pole separation

$$\Delta p=2\gamma_B \tag{3.7c}$$

is pure real. Figure 3 shows a graphical construction whereby Δp can be evaluated as a function of $\delta\Omega$ for given $S\Delta\Omega$ and ϕ. In the complex z plane, the curve

$$\text{Im } z^2=(S\Delta\Omega)^2\sin\phi \tag{3.8}$$

is drawn and the vectors $\pm S\Delta\Omega e^{i\phi/2}$ are indicated. The appropriate Δp is such that $\delta\Omega+i\Delta p$ lies on the curve (3.8). Note that as $|\delta\Omega|$ decreases to $|\delta\Omega_c|=S\Delta\Omega|\cos\frac{1}{2}\phi|$, $\Re$ evaluated from (3.3c) tends to zero. For $|\delta\Omega|<|\delta\Omega_c|$, there is no solution for Δp satisfying the requirement (3.5b) that $\Re$ be real. Thus the premises of the model lead to a contradiction in this range. However, the nonlinear differential-equation techniques described in Sec. 4 indicate that the modes are locked together over the whole range.

The remainder of this section assumes $\delta\Omega$ above the lock-in value, but sufficiently close that $\Re$ is much less than a linewidth, ensuring validity of the assumption that gain is frequency-invariant.

From (3.5b) or from Fig. 3 it is found that

$$\Delta p=(S\Delta\Omega)^2(\sin\phi)/2\delta\Omega, \tag{3.9a}$$

and from (3.3c) that

$$\begin{aligned}\Re&=[\delta\Omega^2-\Delta p^2-(S\Delta\Omega)^2\cos\phi]^{1/2}\\&=\delta\Omega\{[1-r\cos^2(\tfrac{1}{2}\phi)][1+r\sin^2(\tfrac{1}{2}\phi)]\}^{1/2},\end{aligned} \tag{3.9b}$$

where

$$r=(S\Delta\Omega/\delta\Omega)^2. \tag{3.9c}$$

The cases $\phi=0$ and $\phi=\pi$ represent the most extreme situations. For $\phi=0$, $|\delta\Omega_c|=S\Delta\Omega$, and above lock-in,

$$\begin{aligned}\Delta p&=0,\\ \Re&=[\delta\Omega^2-(S\Delta\Omega)^2]^{1/2}.\end{aligned} \tag{3.10a}$$

For $\phi=\pi$, $|\delta\Omega_c|=0$, and for all other $\delta\Omega$,

$$\begin{aligned}\Delta p&=0,\\ \Re&=[\delta\Omega^2+(S\Delta\Omega)^2]^{1/2}.\end{aligned} \tag{3.10b}$$

The transition to $\Re=0$ at $\delta\Omega=0$ is then discontinuous.

With the determination of $\sum p$ and $\Re$, the characteristic frequencies are completely specified:

$$\Omega_{S1}=\Omega_0\pm\tfrac{1}{2}(\delta\Omega-\Re) \tag{3.11a}$$

and

$$\Omega_{S2}=\Omega_0\pm\tfrac{1}{2}(\delta\Omega+\Re). \tag{3.11b}$$

The amplitudes $A_F(\Omega)$ and $A_B(\Omega)$ comprise Dirac δ functions located at the characteristic frequencies:

$$A_S(\Omega)=A_{S1}\delta(\Omega-\Omega_{S1})+A_{S2}\delta(\Omega-\Omega_{S2}). \tag{3.12}$$

Let symbols κ_F and κ_B be defined as

$$\kappa_S=A_{S2}/A_{S'1},$$

and evaluated from the coupled oscillator equations (2.7) and the characteristic frequencies (3.3):

$$\kappa_S=S\Delta\Omega e^{i\phi_{SS'}}/\pm i(\delta\Omega+\Re+i\Delta p). \tag{3.13}$$

In the limit

$$S\Delta\Omega\ll\delta\Omega,$$

κ_F and κ_B tend to zero, indicating that the waves at Ω_{F1} and Ω_{B1} have amplitudes much larger than those at Ω_{B2} and Ω_{F2}. The former will be called *primary* waves, the latter *secondary* waves. The primary amplitudes are such that (3.7b), (3.7c), and (3.9a) are satisfied.

Let κ_F' and κ_B' be defined as

$$\begin{aligned}\kappa_S'&=A_{S2}/A_{S1}\\&=\kappa_S A_{S'1}/A_{S1}.\end{aligned} \tag{3.14}$$

The signals are

$$A_F=A_{F1}(e^{i\Omega_{F1}t}+\kappa_F'e^{i\Omega_{F2}t}), \tag{3.15a}$$

$$A_B=A_{B1}(e^{i\Omega_{B1}t}+\kappa_B'e^{i\Omega_{B2}t}). \tag{3.15b}$$

Consider the time evolution of the phase angle

$$\theta=\measuredangle A_B-\measuredangle A_F \tag{3.16a}$$

between the two modes. From Eqs. (3.15) and the specific values of the characteristic frequencies (3.11) it is found that

$$\begin{aligned}\dot\theta=\Re-\delta\Omega+\frac{d}{dt}[&\measuredangle(1+\kappa_B'e^{-i\Re t})\\&-\measuredangle(1+\kappa_F'e^{i\Re t})].\end{aligned} \tag{3.16b}$$

A curve of $\dot{\theta}$ as a function of time in the special case $\phi=0$, $S\Delta\Omega/\delta\Omega\simeq 0.9$, $A_{F1}=A_{B1}$ is shown in Fig. 4. It coincides *exactly* with the curve of $\dot{\theta}$ computed with nonlinear differential equation techniques described by Wang.[3] (The time origin is, of course, arbitrary.) A curve of $\cos\theta$ as a function of time constructed from (3.16b) displays a distorted, nonsinusoidal shape. Such curves seem to have been predicted first by Adler[16] and subsequently by many others using nonlinear differential equation techniques for problems similar to the laser mode-coupling problem.

Unfortunately neither the instantaneous $\dot{\theta}$ nor $\cos\theta$ can easily be investigated directly. But intensities are readily observed, and will suffice to reveal at least $\mathfrak{R}$, the time-average value of $\dot{\theta}$ in the ring frame. The F and B intensities observed are

$$I_F=1+|\kappa_F'|^2+2|\kappa_F'|\cos(\measuredangle\kappa_F'+\mathfrak{R}t), \quad (3.17a)$$

$$I_B=1+|\kappa_B'|^2+2|\kappa_B'|\cos(\measuredangle\kappa_B'+\mathfrak{R}t). \quad (3.17b)$$

Both are modulated at frequency $\mathfrak{R}$. Modulation of the single beam intensities at the time-average beat frequency between the F and B waves has been observed experimentally.[17,18]

Consider now the total intensity I measured by a detector in the ring frame. Expressed in terms of the total intensities at each of the two frequencies present,

$$I\propto|A_{F1}(1+\kappa_B)|^2+|A_{B1}(1+\kappa_F)|^2 +2|A_{F1}(1+\kappa_B)||A_{B1}(1+\kappa_F)|\cos\alpha, \quad (3.18)$$

where

$$\alpha=\measuredangle A_{B1}(1+\kappa_F)-\measuredangle A_{F1}(1+\kappa_B)+\mathfrak{R}t.$$

Apparently I is a constant combined with a sinusoid with frequency $\mathfrak{R}$ and intensity sensitive to the exact phases ϕ_{FB} and ϕ_{BF}. If either κ_F or κ_B tends to -1, the beat signal effectively disappears. Thus there can appear to be a lock-in even if $\delta\Omega$ is above $\delta\Omega_c$. The indicated superiority of single-beam detection of beat signal at low rotation rate has been observed experimentally.[18]

4. CONNECTION TO NONLINEAR DIFFERENTIAL-EQUATION APPROACH

The mode-coupling problem can be analyzed through the time-domain differential equations

$$dA_F/dt=p_FA_F+\tfrac{1}{2}S\Delta\Omega e^{i\phi_{FB}}A_Be^{+i\delta\Omega t}, \quad (4.1)$$

$$dA_B/dt=p_BA_B+\tfrac{1}{2}S\Delta\Omega e^{i\phi_{BF}}A_Fe^{-i\delta\Omega t}. \quad (4.2)$$

A most extensive study of this differential-equation approach has been undertaken by Wang.[3] Others[4–9] have studied more complicated but essentially equivalent sets of second-order equations. In his analysis, Wang interprets the signals A_S as complex space-time functions $A_S(z,t)$ that have only positive frequency parts when spatially Fourier-decomposed. In this context, the phase shifts are position-dependent:

$$\phi_{SS'}=\phi_{SS'}|_{z=0}\mp 2Kz.$$

The gains contained in p_S depend on $|A_F(t)|$ and $|A_B(t)|$, respectively. In principle, the equations are nonlinear. However, in the low-excitation limit, the gain variations are tiny.

In the preceding sections, (4.1) and (4.2) have essentially been spatially Fourier-decomposed. Steady state defined in terms of the autocorrelations of the spatial amplitudes has been assumed. The equations have then been time-decomposed. In principle, the original gain dependence on $|A_S(z,t)|$ would be manifest as a symbolic gain dependence on Ω, which for simplicity has been neglected. In each mode, two frequencies separated by an amount $\mathfrak{R}$ have been predicted. Actually, infinitesimal pulsations in the excitation density would generate additional infinitesimal signals separated by multiples of $\mathfrak{R}$. These are neglected in the linear model, but not in the nonlinear differential-equation approach. They provide a perturbation on the system's gross behavior predicted by the linear model. Mainly they make the individual A_F and A_B amplitudes fluctuate less in time. Computations[3] show that away from the low excitation limit, the pulsation's effect on $\dot{\theta}$ is (a) nil in the $\phi=0$ case and (b) a slight decrease in time-average value in the $\phi=\pi$ case. In general, the following system of equations is to be solved. Let

$$p_F=i\Omega_0-\gamma_F,$$
$$p_B=i\Omega_0-\gamma_B,$$
$$\chi=\ln|A_F/A_B|,$$
$$\theta=\measuredangle A_B-\measuredangle A_F.$$

Then in inertial space

$$\dot{\chi}=\gamma_B-\gamma_F+\tfrac{1}{2}S\Delta\Omega[|A_B/A_F|\cos(\phi_{FB}+\theta+\delta\Omega t) -|A_F/A_B|\cos(\phi_{BF}-\theta-\delta\Omega t)],$$

$$\dot{\theta}=\tfrac{1}{2}S\Delta\Omega[|A_F/A_B|\sin(\phi_{BF}-\theta-\delta\Omega t) -|A_B/A_F|\sin(\phi_{FB}+\theta+\delta\Omega t)].$$

The equation for $\dot{\theta}$ agrees with that derived by Aronowitz and Collins[2] from fundamental self-consistency considerations. At steady state in the $\phi=0$ case, A_F and A_B maintain equal magnitudes. Equality is predicted also by the linear model, so both models give exactly the same $\dot{\theta}$.

5. CONCLUSION

Although the discussion in this and the preceding paper is limited to ring lasers, the ideas seem applicable to the explanation of effects that have been observed in other systems. Consider, for example, a standing-

[16] R. Adler, Proc. I.R.E. **34**, 351 (1946).
[17] T. J. Hutchings, J. Winocur, R. H. Durrett, E. D. Jacobs, and W. L. Zingery, Phys. Rev. **152**, 467 (1966).
[18] P. Fenster and W. K. Kahn, Electron. Letters **2**, 380 (1966).

wave maser with two modes excited. It is similar to a ring laser viewed in the ring frame. The distinction between F and B modes becomes that between adjacent, oppositely polarized standing-wave modes. The coupling parameter $S\Delta\Omega$ becomes unity, and ϕ_{FB} and ϕ_{BF} become zero. Amplitude modulation, frequency pulling, and locking of the modes are all predicted. Presumably the analysis can be generalized to whatever number of modes is present.

As another example, consider a standing-wave maser supporting one excited mode in a weak axial magnetic field. It, too, is similar to the ring laser viewed in the ring frame. The distinction between F and B becomes that between orthogonal polarizations. The FB frequency difference is caused by birefringence of the medium. Irregular precession and locking of the polarization ellipse are predicted.

Since they can all be predicted quantitatively in terms of a linear model, it is apparent that the phenomena mentioned need not be attributed to the nonlinearities of the laser medium. Instead, nonlinearities are reserved to explain modifications evident at high excitations.

ACKNOWLEDGMENT

The author is indebted to J. D. Coccoli of MIT Instrumentation Laboratory for contributions, and with pleasure acknowledges his help.

APPENDIX A: COUPLED OSCILLATOR EQUATIONS

Consider a linear system with a single pole located in the frequency domain at

$$p=-\gamma_0+i\Omega_0. \tag{A1}$$

This serves as a model of a lossy cavity resonator. Let complex signals be added to the cavity at a rate $a(t)$. The resulting complex field $A(t)$ within the cavity can be obtained in three well-known equivalent ways:

(a) Components in the frequency domain;

$$A(\Omega)=a(\Omega)/(i\Omega-p). \tag{A2a}$$

(b) Response in the time domain;

$$A(t)=\int_{-\infty}^{t} e^{p(t-\tau)}a(\tau)d\tau. \tag{A2b}$$

(c) Field evolution with time;

$$dA(t)/dt=pA(t)+a(t). \tag{A2c}$$

The expression (A2b) results from inverse Fourier-transforming (A2a), Eq. (A2c) results from differentiating (A2b), and Eq. (A2a) results from Fourier-transforming (A2c). Expression (A2a) leads to two useful concepts. For $a(\Omega)=$const., $|A(\Omega)|$ attains $\frac{1}{2}\sqrt{2}$ its maximum value when

$$\Omega=\Omega_0\pm\gamma_0\equiv\Omega_{\pm 1/2}.$$

These values of Ω are commonly referred to as half-power points because $|A(\Omega_{\pm 1/2})|^2$, a measure of energy density, is at half its maximum value. The interval $2\gamma_0$ between half-power points is commonly referred to as the bandwidth $\Delta\Omega$ of the resonator.

Expression (A2b) gives another familiar concept. In one period of oscillation, $2\pi/\Omega_0$, an input increment $a(\tau)d\tau$ decays in energy by the factor

$$-2\pi\Delta\Omega/\Omega_0.$$

The quantity $\Omega_0/\Delta\Omega$ is commonly called the quality factor Q of the resonator.

Expression (A2c) shows that when the input signal is turned off at time t, the rate of energy decay is $\Delta\Omega$.

The introduction of gain into the cavity, such as is produced by laser material, modifies p, to give

$$p\rightarrow-\gamma+i\Omega_0, \tag{A3a}$$

where

$$\gamma=\tfrac{1}{2}(\Delta\Omega-G), \tag{A3b}$$

with the gain G expressed in frequency units. The gain G depends on field amplitudes, so the system represented by (A2c) has become nonlinear. It is no longer strictly correct to call p the location of a "pole" or to describe the system by (A2a) or (A2b). However, within the limits indicated in the paper, linear system theory can provide useful information about such a system.

APPENDIX B: FREQUENCY SHIFTS AT A MOVING MIRROR

In principle, the frequency shift experienced by a backscattered beam is computed by transforming the frequency from inertial space to the rotating ring frame, reversing the beam, and transforming the frequency back to inertial space. The required transformations can be computed by considering the equivalent circular ring,[19,20] which has radius R determined as twice the ring area divided by its inertial-space optical path length.

Neglecting dispersion, light travels at speed c in inertial space. It follows that the F and B times taken to traverse distance $Rd\phi$ in the rotating circular ring are

$$dt_S=Rd\phi/(c\mp R\omega_r).$$

The invariance of absolute phase from frame to frame implies that frequency transformations are as follows.

To convert Ω from inertial space to the ring frame, multiply by:

$$F \text{ wave}, \quad (c-R\omega_r)/c;$$
$$B \text{ wave}, \quad (c+R\omega_r)/c.$$

[19] J. D. Coccoli and D. A. Koso, MIT Instrumentation Laboratory Report No. E-1943, 1966 (unpublished).
[20] E. O. Schulz Dubois, IEEE J. Quantum Electron. **QE2**, 299 (1966).

To convert Ω from the ring frame to inertial space, multiply by:

$$F \text{ wave}, \quad c/(c-R\omega_r);$$
$$B \text{ wave}, \quad c/(c+R\omega_r).$$

When F radiation with frequency Ω_F is backscattered, it appears in the B mode with frequency $\Omega_F(c-R\omega_r)/(c+R\omega_r)\simeq\Omega_F(1-2R\omega_r/c)$. Similarly, B radiation appears in the F mode with frequency $\simeq\Omega_B(1+2R\omega_r/c)$. In the ring laser, all frequencies present are very near the cavity resonant frequency, so all frequency shifts are approximately of magnitude $|\delta\Omega/\Omega_0|\simeq 2R\omega_r/c$. Note that if the ring were a regular polygon, this formula could have been computed as the first-order approximation to the Doppler shift experienced by a wave backscattered from a mirror moving with the ring instantaneously but not accelerating with it. However, the Doppler formula would not be correct to higher orders in the mirror velocity, and would not even be applicable for a general irregular polygon, where different mirrors lie at different radii from the rotation axis.

APPENDIX C: LASER GAIN

At steady state, the laser gain $G_S(\Omega_0,\Omega)$ for each of the four frequencies Ω_{S1}, Ω_{S2} present equals half the corresponding energy loss rate, which is ϵ_0^{-1} times a fictional conductivity $\sigma_S(\Omega_0,\Omega)$, which in turn is given by a self-consistency equation derived in the preceding paper. Neglecting pulsations in the excitation density, it is found that

$$\epsilon_0^{-1}\sigma_S(\Omega_0,\Omega)=G_S(\Omega_0,\Omega)=\frac{\Omega|\mu_{ab}|^2}{2\epsilon_0\hbar\gamma}\int_v N(v)e^{\mp\mu}\mathcal{L}_S,$$

where the various symbols are defined in the preceding paper.

PHYSICAL REVIEW VOLUME 181, NUMBER 2 10 MAY 1969

Channeling of MeV He^+ Ions in Tungsten and Other Crystals: An Intercomparison of Rutherford Scattering and of Characteristic L and M X-Ray Yields

J. A. DAVIES, L. ERIKSSON,* N. G. E. JOHANSSON,* AND I. V. MITCHELL
Chalk River Nuclear Laboratories, Chalk River, Ontario, Canada
(Received 13 May 1968; revised manuscript received 14 January 1969)

Measurements of wide-angle (150°) scattering and of L and M x-ray yields in tungsten single crystals are reported as a function of crystallographic orientation with respect to an incident beam of 1.4-MeV helium ions. Comparison of these yields establishes both lower and upper limits for the minimum impact parameter ($r_{\min}$) between a channeled ion and the tungsten-lattice atoms; these limits are consistent with Lindhard's estimate that $r_{\min}\sim\mathbf{a}$, the Thomas-Fermi screening distance (i.e., $\sim$0.11 Å for He in W). A similar comparison between wide-angle scattering and x-ray yield curves is reported for several other lattices—Al, Si, GaP, GaSb, and UO_2; again the results are consistent with the predicted relationship: $r_{\min}\sim\mathbf{a}$. Anomalies in published orientation studies of K, L, and M x-ray yields are shown to be due to depth effects.

I. INTRODUCTION

PREVIOUS theoretical[1] and experimental[2,3] work has established that close-encounter processes such as wide-angle Rutherford scattering exhibit extremely strong attenuations whenever the incident beam is aligned within a predicted critical angle of a major axis or plane. For example, in tungsten along a major axis such as the ⟨111⟩, attenuation factors of up to 100 have been observed, indicating that as much as 99% of the incident beam is being channeled on entering the crystal. These earlier Rutherford-scattering measurements can be used to establish upper and lower limits to $r_{\min}$. On the one hand, for the channeled fraction to be as large as 99%, the "forbidden" area $\pi(r_{\min})^2$ around each atomic row must be less than 1% of the available area. This sets an upper limit of 0.13 Å for $r_{\min}$ in the case of ⟨111⟩ tungsten. On the other hand, the existence of such a strong orientation dependence also requires that $r_{\min}$ cannot be less than $\bar{p}$ where $\bar{p}$ is the impact parameter of the particular close impact process. For wide-angle Rutherford scattering of MeV projectiles, $\bar{p}$ is typically 10^{-3}–10^{-4} Å; hence, these upper and lower limits for $r_{\min}$ are about two orders of magnitude apart.

In order to establish narrower experimental limits for $r_{\min}$, we need to investigate the orientation dependence of processes for which $\bar{p}$ is much larger than 10^{-3} Å. For this purpose, the characteristic inner-shell x-ray yields are particularly suitable, since they cover the desired range of impact parameters. Unfortunately, a quantitative relationship between the mean radius of

* Permanent address: Research Institute for Physics, Stockholm 50, Sweden.

[1] J. Lindhard, Kgl. Danske Videnskab. Selskab, Mat.-Fys. Medd. **34**, 14 (1965).

[2] E. Bøgh and E. Uggerhøj, Nucl. Instr. Methods **38**, 216 (1965).

[3] J. A. Davies, J. Denhartog, and J. L. Whitton, Phys. Rev. **165**, 345 (1968).